Available online at www.sciencedirect.com
SCIENCE DIRECT®
Estuarine, Coastal and Shelf Science 61 (2004) 65–71
ESTUARINE COASTAL AND SHELF SCIENCE
www.elsevier.com/locate/ECSS

Fractal analysis of shoreline patterns for crenulate-bay beaches, Southern China

Zhi-Jun Dai[a,b,*], Chun-Chu Li[b], Qing-Ling Zhang[c]

[a]State Key Lab of Estuarine & Coastal Research, East China Normal University, Shanghai, 200062, PR China
[b]Institute of Estuarine and Coastal Research, Zhongshan University, GuangZhou, 510275, PR China
[c]Geography Department, Central Michigan University, Mount Pleasant, 48858, MI, USA

Received 9 June 2003; accepted 5 April 2004

Abstract

Shoreline patterns of 34 crenulate-bay beaches in Southern China were investigated. The differentiated criteria for log-spiral shoreline curves offered by Silvester (Am. Soc. Civ. Eng. Proc. 96 (1970) 275; Coastal Engineering, Elsevier, Amsterdam (1974) 338) and Hsu et al. (J. Waterw. Port Coast. Eng. 115 (1989) 285) were used to determine the equilibrium morphology of each beach. Results show that the discriminated principles of the equilibrium log-spiral curve were not suitable for all the beaches. Based on the theory of the log-spiral stable curve and beach morphology and the dynamic action setting in Southern China, fractal analysis was adopted to classify the patterns in the shorelines. It shows that shorelines include three modes: dynamic balance of accretion, static equilibrium and the dynamic balance of erosion.

Keywords: fractal analysis; log-spiral theory; shoreline patterns; crenulate-bay beach

1. Introduction

Crenulate-shaped bays are quite common on exposed sedimentary coasts (Hsu et al., 1989). Bay shapes have received various names, such as half-heart shaped (Silvester, 1960), headland-bay beaches (LeBlond, 1979; Wong, 1981), crenulate-shaped bays (Silvester and Ho, 1972), curved or hooked beaches (Rea and Komar, 1975), and zeta bays or pocket beaches (Silvester et al., 1980), etc. Crenulate-bay beaches occur with the presence of two consecutive headlands and a predominant wave approach oblique to the alignment of the upcoast and downcoast headlands (Silvester, 1970). Oblique persistent swell striking a shoreline transports sediment alongshore and sculptures a headland-dominated coast into crenulate-shaped bays (Finkelstein, 1982). Arc-shaped or spiral-shaped bay beaches in Southern China are one of the typical examples of this kind (Fig. 1).

The stable physiographic feature of crenulate-shaped bays was recognized by Jennings (1955). Numerous theoretical studies concerning crenulate-bay beach morphology have been carried out since Yasso (1965), who examined the plan forms of a number of prototype bays and reported their equivalence to the logarithmic spiral (see Silvester, 1970, 1976; LeBlond, 1972). Theoretically, a crenulate bay may be formed in response to an updrift headland and its beach will take the shape of a logarithmic spiral (Finkelstein, 1982). Later, using computer simulation of a hooked beach, some investigators have found that its equilibrium configuration is governed by the pattern of offshore wave refraction and diffraction, and the distribution of wave energy governs the equilibrium configuration (Silvester, 1970, 1974, 1976; Rea and Komar, 1975). Once a stable equilibrium curve on a shoreline is formed, wave refraction and diffraction orthogonally approach the shore as normal, wave crests break simultaneously, and alongshore sediment transport ceases. However, a bay out of equilibrium or in dynamic equilibrium will have waves break at some angle to the shore, resulting in sediment transport through the bay. Thus, it is possible to distinguish between crenulate bays in full equilibrium where alongshore drift has ceased and those not having yet reached

* Corresponding author.
E-mail address: zhijun_dai@hotmail.com (Z.-J. Dai).

0272-7714/$ - see front matter © 2004 Elsevier Ltd. All rights reserved.
doi:10.1016/j.ecss.2004.04.004

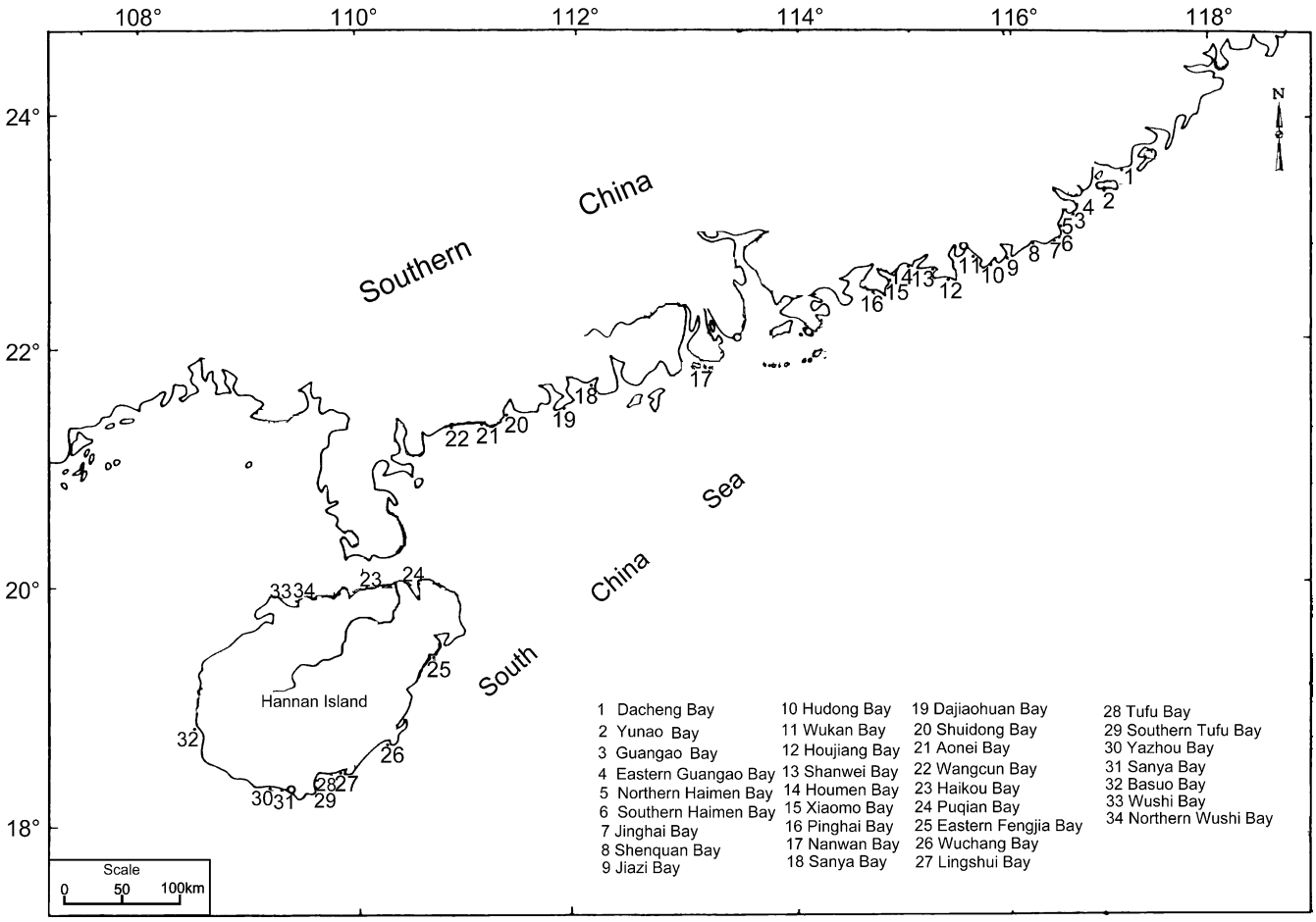

Fig. 1. Thirty-four crenulate-bay locations in Southern China.

their stability (Silvester, 1974). According to the theory of the spiral-shaped curve, Silvester (1970, 1974) and Hsu et al. (1989) both developed a methodology to generate a best-fitted curve to shorelines of this type to determine whether they are in equilibrium or not (Figs. 3–5). The methods are as follows. The predominant wave approach angle for each crenulate-bay beach is first determined. The logarithmic spiral may then be resolved and used as equilibrium overlay (Fig. 3). Zones of erosion and deposition are predicted as the equilibrium logarithmic spiral is placed over the original crenulate-bay shoreline (Silvester, 1974). Silvester and Ho (1972) also demonstrated that the ratio of the indentation length, a, to clearance between headlands, b, may be used to determine if a crenulate bay is in equilibrium (Fig. 4). Later, Hsu et al. (1989) showed other methods to estimate whether or not a crenulate bay is in equilibrium (Fig. 5).

This paper discusses first whether or not the above methods are suitable to determine if a crenulate-bay shoreline in Southern China is in an equilibrium state. A discussion on the shortage of traditional methods is useful here for understanding the aim of this study. Based on fractal analysis, a crenulate-bay beach model was developed which takes into account the theoretical aspects about the formation of crenulate bays in Southern China.

1.1. Study area

Thirty-four crenulate bays in Southern China were investigated to obtain information on the arc-shaped shoreline. These bays were selected because of their characteristic crenulate shapes and because their lengths that exceed 4 km. The localities for them are shown in Fig. 1.

Coastlines are dominated by rocky headlands at the mouths of deeply incised valley and estuary bays. Prevailing weather conditions are largely determined by an anti-cyclonic belt. High-pressure systems are periodically displaced by tropical and sub-tropical cyclonic depressions or locally modified by sea-breeze activity. This basic seasonal rhythm is modified by other weather systems, particularly by afternoon sea breezes which blow onshore during summer days and offshore in winter days. The strong seasonality of the weather regime directly affects the regional wave climate. The Southern China Coast is dominated by a low to

moderate energy deep-water wave regime characterized by persistent south to southeast swell. The wave climate is mild, with an average significant wave height of 1.1 m. Wave heights of more than 4 m often occur when tropical or sub-tropical cyclonic depressions pass by this region. There is little variation in the low wave energy from year to year from summer to autumn period. However, the wave climate is more severe in winter and spring period as the cold air from North China controls the Southern China region. Average tidal ranges less than 1 m in are common in the Southern China Coast. Due to the relatively low tidal ranges, this region is largely dominated by wave effects.

2. Data acquisition and methodology

2.1. Plan shape data gathering

Silvester (1970, 1974) and Hsu et al. (1989) proposed a new approach to estimate whether or not a crenulate bay is in equilibrium. They demonstrated that the curved segment of an equilibrium crenulate bay generally follows a logarithmic spiral. Therefore, log-spiral curves can be used to determine the future shape of a crenulate bay (Finkelstein, 1982). According to this method, the plan shape data of 34 bays were obtained from the contour charts and sea maps with a scale of 1 cm to 500 m (1:50000). Plan shape data include the log-spiral constant angle α, the largest indentation a, the predominant wave crests to the control line of length b and its angle β, and the ratios of radius R to its angle θ (Fig. 2, Table 1). The 34 bays studied in detail are plotted in Figs. 3–5. The Wangcun Bay $\beta^{0.83}/\theta^{0.77}$, whose value is 0.128, is too small to plot in Fig. 3.

2.2. Fractal method and data acquisition

Fractals have been given a formal mathematical definition (Mandelbrot, 1982). However, an intuitive definition should be more useful: in a geometrical fractal the part is reminiscent of the whole. This implies that the system is self-similar and scale-invariant, i.e., its morphology repeats itself at various length scales. This means that small pieces of the system can be magnified to obtain its structure at larger length scales (Sahimi, 2000). Thus, fractal analysis can be performed to describe the complexity, chaos and un-regulation of the geomorphology or other system by estimating the statistical fractal dimension (D) (Feder, 1988), defined as follows.

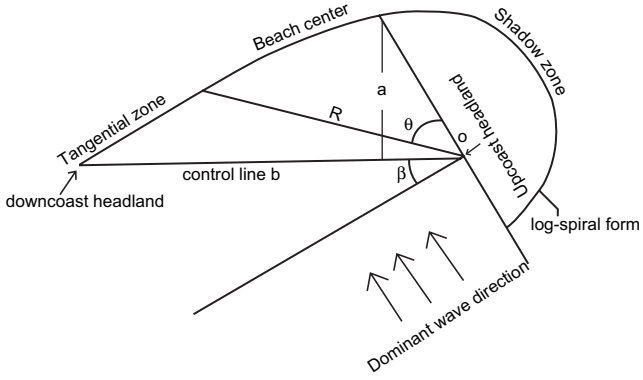

Fig. 2. Definition sketch for bay in static equilibrium.

The fractal system was covered by non-overlapping d-dimensional hyperspheres of Euclidean radius r, and by counting the number $N(r)$ of the spheres, which is required for its coverage. For a fractal system:

$$N(r) \sim r^{-D} \tag{1}$$

where $\sim$ implies an asymptotic proportionality. Eq. (1) can be rewritten as:

$$D = \frac{\ln N}{\ln(\frac{1}{r})} \tag{2}$$

Thus, for Euclidean objects such as straight lines, squares, or spheres, $N(r) \sim r^{-1}$, $N(r) \sim r^{-2}$, $N(r) \sim r^{-3}$, respectively, and their D coincides with the Euclidean dimension d. Another way for defining and estimating D is to consider a segment of a fractal system of linear dimension L by denoting its volume $V(L)$ as L is varied. If $V(L)$ is calculated by covering the system by spheres of radius unity, then $V(L)$ equals $N(L)$, where N is the number of such spheres required to cover the system. In a fractal system, Sahimi (2000) proposed to calculate D using Eq. (3), which is called the box-counting method:

$$N(L) \sim L^{-D} \tag{3}$$

There are a number of methods available for fractal dimension estimation (Mandelbrot, 1982). In this study, the box-counting method is chosen because it is much more performable and applicable for patterns with or without self-similarity (Legendre et al., 1994). According to this method, each map containing a crenulate bay is covered by a sequence of grids of descending sizes and then two values are recorded for each of the grids, i.e., the number of sequence boxes intersected by the map, $N(r)$, and the side length of the squares, r. All the dots of the value of $N(r)$ and corresponding to r are plotted on the log–log figure, the slope of a curve from points to points, while the correlation value (R) is achieved by linear regression of the dots (Table 1). The value of slope from the straight line is D.

According to the above mentioned method, values D and (R) for the 34 bays were obtained as listed in Table 1. Log-spiral curve can be used to determine the future shape of a crenulate bay, while D value of the logarithm's spiral line, known as a static equilibrium curve, can also be attained ($D = 1.165$).

Table 1
Plan factors for 34 crenulate bays in Southern China

Preface location	a (km)	b (km)	a/b	β (°)	α (°)	R (km)	R/b	$\beta^{0.83}/\theta^{0.77}$	D	(R)
1	2.75	11.75	0.23	43	40	8.7	0.74	0.472	1.197	0.997
2	1.5	4.8	0.31	58	25	1.8	0.375	0.319	1.113	0.999
3	5.5	14.75	0.37	62	50	9.1	0.617	0.568	1.202	0.999
4	1.9	4.7	0.40	60	15	2.75	0.585	0.209	1.15	0.99
5	3.45	9.75	0.35	60	50	5.6	0.574	0.568	1.025	0.99
6	2.1	9.0	0.23	38	50	2.2	0.244	0.568	1.025	0.99
7	1.6	4.3	0.37	50	40	2.0	0.465	0.472	1.103	0.99
8	2.6	13.5	0.19	35	30	3.2	0.237	0.372	1.013	0.99
9	2.75	9.25	0.30	60	40	3.7	0.4	0.472	1.087	0.99
10	1.35	4.7	0.29	50	40	1.5	0.32	0.472	1.086	0.99
11	3.8	14.75	0.26	45	25	3.8	0.258	0.319	1.062	0.998
12	2.75	7.255	0.38	55	30	3.5	0.482	0.372	1.015	0.99
13	4.75	10.8	0.44	55	35	6.3	0.583	0.423	1.027	0.99
14	0.85	4.1	0.21	40	40	2.1	0.512	0.472	1.018	0.994
15	1.2	5.5	0.22	40	30	1.7	0.309	0.372	1.399	0.995
16	4.3	9.4	0.46	62	30	6.3	0.670	0.372	1.191	0.999
17	1.3	4.1	0.32	50	25	1.5	0.366	0.319	1.071	0.999
18	5.8	13.25	0.44	60	40	7.1	0.536	0.472	1.177	0.999
19	1.3	4.0	0.33	45	40	1.6	0.40	0.472	1.331	0.987
20	5.0	12.3	0.41	45	45	5.57	0.453	0.521	1.202	0.999
21	0.85	3.5	0.24	35	32	0.9	0.257	0.393	1.198	0.993
22	1.25	6.25	0.20	30	30	0.8	0.128	0.372	1.106	0.994
23	5.5	12.5	0.44	50	27	7.0	0.56	0.341	1.201	0.999
24	7.1	20.0	0.35	40	27	7.8	0.39	0.341	1.168	0.999
25	2.7	5.75	0.47	60	40	2.8	0.487	0.472	1.232	0.997
26	4.8	14.0	0.33	34	33	5.0	0.357	0.403	1.156	0.995
27	3.25	11.0	0.30	42	20	3.4	0.309	0.265	1.201	0.996
28	3.8	9.9	0.38	50	40	5.5	0.556	0.472	1.165	0.998
29	1.7	5.0	0.34	55	15	2.2	0.44	0.209	1.159	0.996
30	3.7	14.3	0.26	40	40	3.6	0.252	0.472	1.11	0.999
31	6.0	15.25	0.40	50	45	7.3	0.478	0.521	1.059	0.999
32	3.2	12.1	0.26	45	35	5.1	0.422	0.423	1.153	0.995
33	3.3	10.1	0.33	30	35	3.2	0.317	0.423	1.221	0.995
34	2.8	10.1	0.28	30	35	2.0	0.20	0.41	1.145	0.997

Abbreviations (see also Fig 2 and text): a = indentation length (km); b = clearance between headlands (km); β = wave crest angle; α = Log-spiral constant angle; R = radius (km); θ = radius angle; (R) = correlation value.

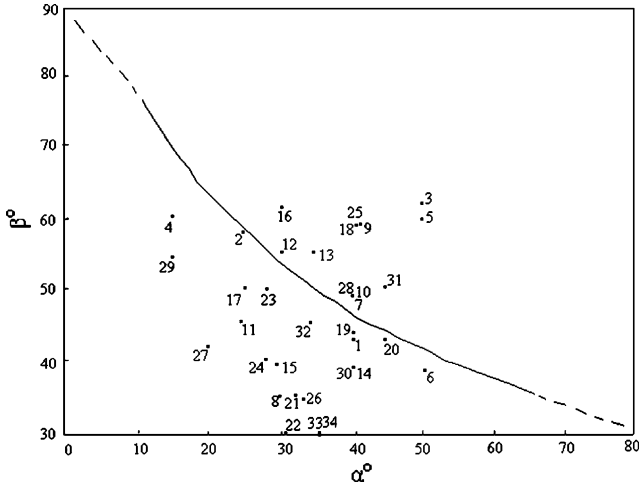

Fig. 3. An equilibrium curve for a specific spiral constant α and β is shown. α and β angles for 34 crenulate bays are plotted. Adapted from Silvester (1974).

3. Results

According to the distinguished standard of an equilibrium spiral curve proposed by Silvester (1970, 1974) and Hsu et al. (1989), Figs. 3–5 show that most of the 34 bays in Southern China can be considered in dynamic equilibrium or in static equilibrium. Moreover, the analyses also show that by the different standards of equilibrium curves of a crenulate bay, the situation of each bay in Southern China is different. Only Bay 7 and Bay 20 just fit for all determined equilibrium standards.

Clearly, even if the methods could be used to evaluate whether or not a shoreline is in static equilibrium, they are not applicable to the coastline of a crenulate bay in Southern China. In fact, these standards were obtained from a laboratory model and corrected by prototype condition. However, the tested field data originated from the small bay or arc-shaped shoreline along an island where little littoral drift and fluid transparent sediment is common. Conversely, although the rock projected to sea in Southern China, littoral drift is

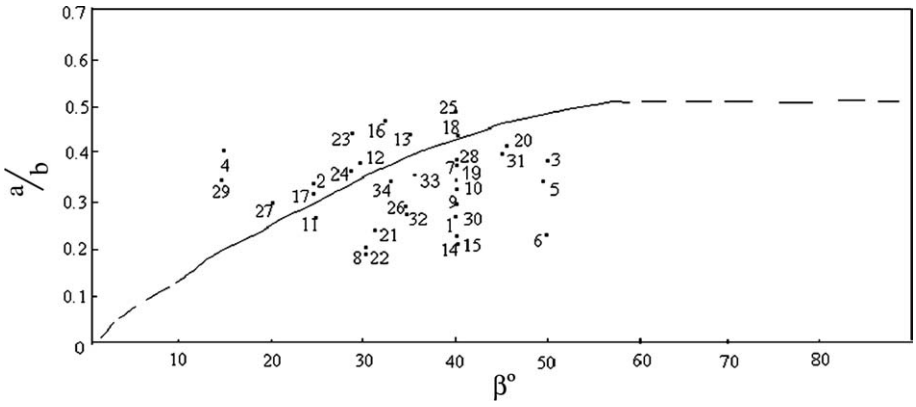

Fig. 4. An equilibrium curve for a specific spiral constant angle β and indentation ratio (a/b) is shown. β and a/b for the 34 crenulate bays are plotted. Adapted from Silvester and Ho (1972).

obstructed and most of the arc-shaped bays form closed systems. There is a tidal inlet in the shadow zone for most of the bays, through which lots of materials pass across the bay, conditions under which sediment transporting occur become much more complex. Thus, it is impossible to study these stable bays having sediment supply by using equilibrium criteria.

4. Discussion

Fractals are generally self-similar and scale-independent. Nature conforms to fractals much more than it does to classical shapes. Therefore, fractals can serve as models for many natural phenomena (Foroutan-pour et al., 1999). Application of fractal theory allows description of various fragmenting and branching states in biological, ecological and other systems (Burrough, 1981; Critten, 1997; Legendre et al., 1994; Milne, 1998).

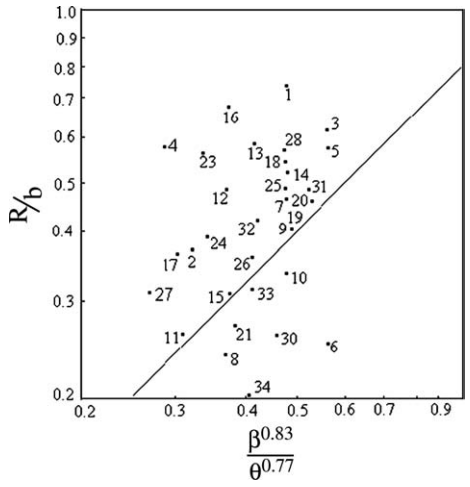

Fig. 5. An equilibrium curve of arc ratio R/b versus parameter $\beta^{0.83}/\theta^{0.77}$ is shown. R/b and $\beta^{0.83}/\theta^{0.77}$ for the 34 crenulate bays studied are plotted. Adapted from Hsu et al. (1989).

Fractal concepts have provided a new approach for quantifying the geometry of complex or noisy shapes and objects (Foroutan-pour et al., 1999). Thus, a crenulate-bay shape could be explained and quantified by the fractal theory.

Based on the log-spiral theory, the log-spiral curve was adopted to determine the future morphological change of a crenulate bay. Thereby, in comparison with the fractal value of the log-spiral curve, fractal values of 34 crenulate bays can be classified into three kinds (Table 2): (1) $D < 1.165$, (2) $D = 1.165$, and (3) $D > 1.165$. Table 2 shows that only Bay 28 is in static equilibrium. It is obvious that the static equilibrium for the shoreline is rare in nature. Further analyses about the morphology and dynamic environment of each kind of bay show that:

(1) In the crenulate bay with D value less than 1.165, the acute angle is formed between wave orthogonal and the shoreline of the shadow zone. The condition of the shadow zone of the bay can develop a hooked spit under the prevailing wave-spread direction, and the predominant drift direction along the shoreline is from the shadow zone to tangent zone. Furthermore, the indentation ratio for these bays is smaller than that for a logarithm spiral curve (Fig. 6A). Since the log-spiral curve is the trend for a crenulate-bay's future development (Silvester, 1970, 1976), shorelines of these bays would recede under the wave action and tend to form a log-spiral curve if there are not enough sediment

Table 2
The balance state for bays in Southern China (see also Fig. 6)

Criteria	Balance state	Crenulate bay in Southern China
$D < 1.165$	The dynamic balance of erosion	2, 4, 5, 6, 7, 8, 9, 10, 11, 12, 13, 14, 17, 22, 26, 29, 30, 31, 32, 34
$D = 1.165$	Static equilibrium (near equilibrium)	28
$D > 1.165$	The dynamic balance of accretion	1, 3, 15, 16, 18, 19, 20, 21, 23, 24, 25, 27, 33

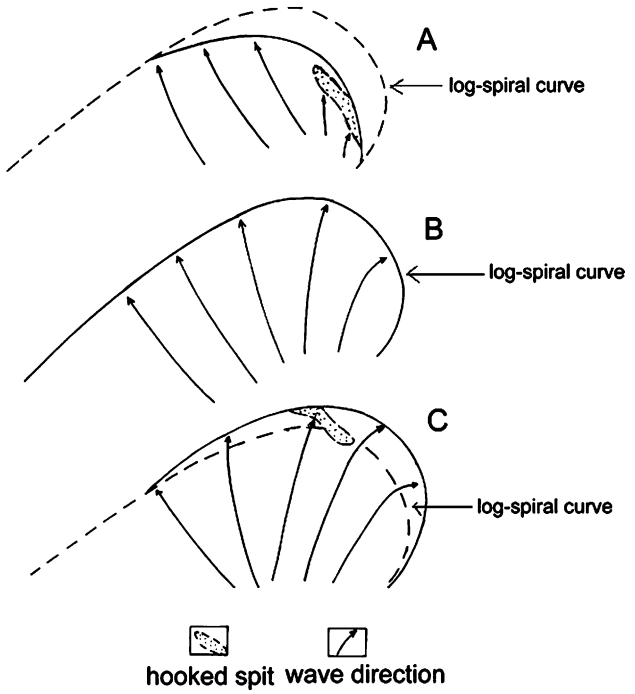

Fig. 6. Shoreline situation for crenulate-bay classification. (A) $D < 1.165$, erosion; (B) $D = 1.165$, equilibrium; (C) $D > 1.165$, accretion.

sources available. Meanwhile, although erosion is common in coastlines over the world, the erosion rates for most of them are so small that people are aware of the balance between the erosion and deposition of the coast. Thus, it is certain that these bays can be said to be in a dynamic balance of erosion.

(2) The static equilibrium: these kinds of bays are similar to those having the log-spiral curve with $D = 1.165$. When incoming waves are refracted and diffracted into the bay, breaking will occur simultaneously along the whole periphery shoreline in the shadow zone, with no sand spit and no littoral drift along shoreline (Fig. 6B).

(3) For bays with $D > 1.165$, the indentation ratio for these bays is greater than the indentation ratio for a logarithm spiral curve. In the shadow zone of such a bay, there will be hooked spits against the prevailing wave direction. Furthermore, locality of the hooked spits is regarded as boundary. In the nearshore areas from the spits to downcoast direction exists net drift along the shoreline (Fig. 6C). In contrast, to bays with $D < 1.165$, the shoreline would be aggraded by the wave action, the sediment tends to fill up space between a crenulate bay and a log-spiral curve if bay environment has enough sediment source. Thus, these kinds of bays may be regarded to be in dynamic balance of accretion.

D values may be considered as a good criterion to quantify the development of coastline. If a coastline had been evolved from a dynamic balance of erosion to static equilibrium, the coast could be in erosion, and its D value could increase. On the other hand, if the coastline had been evolved from a dynamic balance of accretion to static equilibrium, the coast could be in accretion, and its D value may decrease.

5. Conclusions

Based on the theory and methods of the log-spiral equilibrium curve and fractal analysis, estimations of shoreline balance states of crenulate bays were performed and some conclusions can be summarized as follows:

(1) Although the equilibrium criteria (Silvester, 1970, 1974; Hsu et al., 1989) have been extensively applied to many coast regions all over the world, they cannot be applied to the crenulate bays in Southern China.

(2) Fractal analysis can be used to determine what situation the shoreline of a crenulate bay is in. In addition, combined with detailed morphology of the coast zone, D values can be used to define different net sediment transport paths.

(3) Based on prototype data and D values for the tested 34 crenulated bays and the theory for determining whether a logarithm spiral curve is an equilibrium state curve, a fractal analysis can divide the shoreline of crenulate bays into types of dynamic balance of accretion, static equilibrium and the dynamic balance of erosion.

Although fractal analysis is useful and fruitful in determining whether or not bays in Southern China are under erosion or in accretion, morphology and dynamical action settings for a crenulate bay must also be taken into account.

Acknowledgements

This study was supported by Guangdong Province Nature Fund Committee (contract number: 011181). Thanks are also given to our colleagues Xi-Qing Chen and Zhi-Long Li for their help.

References

Burrough, B.B., 1981. Fractal dimensions of landscapes and other environmental data. Nature 294, 240–242.

Critten, K.L., 1997. Fractal dimension relationships and values associated with certain plant canopies. Journal of Agricultural Engineering Research 67, 61–72.

Feder, J., 1988. Fractals. Plenum Press, New York, 283 pp.

Finkelstein, K., 1982. Morphological variations and sediment transport in crenulate-bay beaches, Kodlak Island, Alaska. Marine Geology 47, 261–281.

Foroutan-pour, K., Dutilleul, P., Smith, D.L., 1999. Advances in the implementation of the box-counting method of fractal dimension estimation. Applied Mathematics and Computation 105, 195–210.

Hsu, J.R.C., Silvester, R., Xia, Y.M., 1989. Static equilibrium bays: new relationships. Journal of Waterways, Port, Coastal and Ocean Engineering 115, 285–311.

Jennings, J.N., 1955. The influence of wave action on coastal outline in plan. Geography 6, 36–44.

LeBlond, P.H., 1979. An explanation of the logarithmic spiral plan shape of headland bay beach. Journal of Sediment Petrology 49, 1093–1100.

LeBlond, P.H., 1972. On the formation of spiral beaches. Proceeding of 13th Conference on Coastal Engineering, American Society of Civil Engineering 2, 1331–1345.

Legendre, F.H.P., Bellehumeur, C., Lafrankie, J.V., 1994. Diversity pattern and spatial scale: a study of a tropical rain forest of Malaysia. Environmental and Ecological Statistics 1, 265–286.

Mandelbrot, B.B., 1982. The Fractal Geometry of Nature. W.H. Freeman, New York, pp. 1–486.

Milne, B.T., 1998. Measuring the fractal geometry of landscapes. Applied Mathematics and Computation 27, 67–79.

Rea, C.C., Komar, P.D., 1975. Computer simulation models of a hooked beaches shoreline configuration. Journal of Sediment Petrology 45, 866–872.

Sahimi, M., 2000. Fractal-wavelet neural-network approach to characterization and up-scaling of fractured reservoirs. Computers & Geosciences 26, 877–905.

Silvester, R., 1960. Stabilization of sedimentary coastlines. Nature 188, 467–469.

Silvester, R., 1970. Growth of crenulate shaped bays to equilibrium. Journal of Waterways Harbors and Coastal Engineering, American Society of Civil Engineering, Proceedings 96, 275–287.

Silvester, R., Ho, S.K., 1972. Use of crenulate shaped bays to stabilize coasts. Proceeding of 13th Conference on Coastal Engineering, American Society of Civil Engineering 2, 1347–1365.

Silvester, R., 1974. Coastal Engineering, vol. II. Elsevier, Amsterdam, 338.

Silvester, R., 1976. Headland defense of coasts. Proceeding of 15th Conference Coastal Engineering, American Society of Civil Engineering 2, 1394–1406.

Silvester, R., Tsuchiya, Y., Shibano, T., 1980. Zeta bays, pocket beaches and headland control. Proceeding of 17th International Conference on Coastal Engineering 2, 1306–1319.

Wong, P.P., 1981. Beach evolution between headland breakwaters. Shore and Beach 49, 3–12.

Yasso, W.E., 1965. Plan geometry of headland bay beaches. Journal of Geology 78, 703–714.